

Combustion Engine Analyses Using New and Extended Features in LS-DYNA

Fredrik Bengzon¹, [Anders Jonsson](#)¹, Thomas Borrvall¹

¹Dynamore Nordic AB, Ansys LST

1 Introduction

Recently, many enhancements have been made to LS-DYNA's implicit solver with regard to improved robustness and general functionality. New material models, element formulations, and features for convenient load history management all contribute to making the implicit solver more versatile and user friendly. The new features are of course relevant to general analyses, but here a case-study of a combustion engine analysis is presented to illustrate and promote these new features. Focus will be on thermal and mechanical analyses, to evaluate deformation, stress, plastic strain, gasket pressure etc. The built-in fatigue analysis capabilities of LS-DYNA will also be demonstrated since fatigue life is often the design target in structural analyses of combustion engines.

The present work is not aimed at exactly capturing the properties of an existing combustion engine. The material data, see Section 2.2, is in most cases estimated from various sources, not obtained through proper material testing. The thermal and mechanical loading (see Section 3) are only roughly estimated. Hopefully, these components can make up a somewhat realistic case for demonstrating new features of LS-DYNA implicit on a full-scale example. Since long, LS-DYNA holds a strong position within the automotive industry, as the market leading software for crash and safety analyses, using the explicit solver. Hopefully, this contribution can demonstrate the capabilities of the implicit solver within engine/drivetrain analyses which is quite new to LS-DYNA.

Previously presented work where LS-DYNA is applied to combustion engine analyses include a benchmark of dynamic analysis of an oil sump [2] and the Rolls-Royce jet engine [3]. The complete machinery simulations of rock drills presented in Ref. [7] shows some similarities to combustion engine analyses, involving many moving parts and contacts, various types of pre-tension etc.

The analysis illustrates the multistage concept, originally described in Ref. [4], by combining `*CASE` and `dynain.lsd` to describe the loading sequence as a series of stages. This concept is very convenient for analyses of a sequence of load stages as a sequence of separate but sequentially dependent analyses (see also Appendix B of Ref. [6] and the coming Appendix X of Ref. [5]).

A historical background to structural analysis of combustion engines is presented in Ref. [1]. This gives an interesting overview of the development of powerful tools for FE-analyses of combustion engines during the last 45 years.

2 Model overview

2.1 FE-mesh

For the present demonstrational purposes, a CAD geometry [10] of a four-cylinder in-line engine was used as a basis for creating the FE-model, see the left image of Fig.1:. The CAD modelling work of Mr. Artem Slyusarev gratefully acknowledged. Some modifications and additions to the original model were made, for it to be useful for the present purposes. A subset of parts was kept for the FE-analysis: the oil sump, engine block, cylinder liners, cylinder head, valve cap, exhaust, and intake manifolds, with related connections (gaskets and bolts). The mesh was created using ANSA [11]. For fully parametrized generation of hexahedral representation of bolts, the Connection Manager of ANSA is very useful. In total, the model has 79 bolts, including pre-tensioning (see further Section 3). The model consists of about 3.9E6 nodes and 2.46E6 elements, with a characteristic mesh size of about 5 mm, see the right image of Fig.1:, Fig.2: and Table 1: for details.

Table 1: Number of entities in the FE-model

Entity type	Count
Nodes	3863630
Elements	2406553
2 nd order tet	2280145
1 st order hex	109482
Parts	33

The new enhanced strain hexahedral element with incompatible modes (solid element formulation -18) is used in the cylinder liners and the front spacer plate, see Fig.2:. Solid cohesive elements (formulation 19) were used for the cylinder head gasket, oil sump and exhaust gaskets.

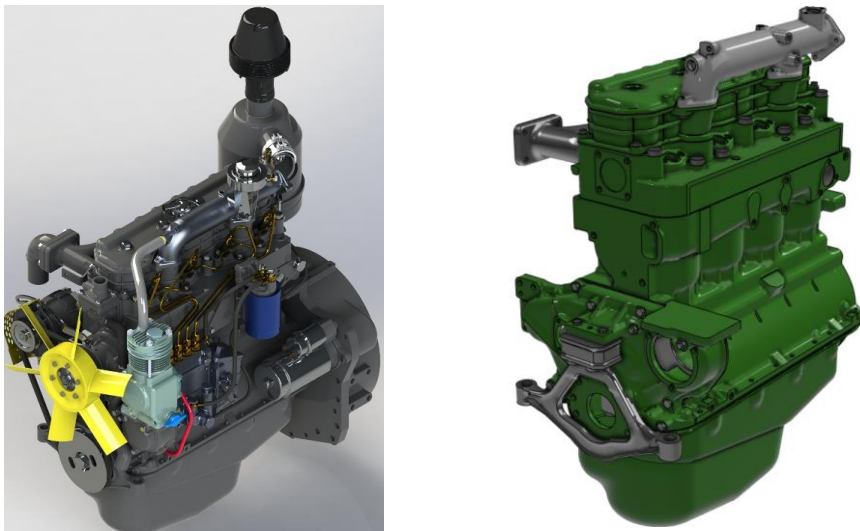


Fig.1: The left image shows the original CAD model. The CAD modelling work of Mr. Artem Slyusarev gratefully acknowledged. The right image shows the FE-model of the kept parts.

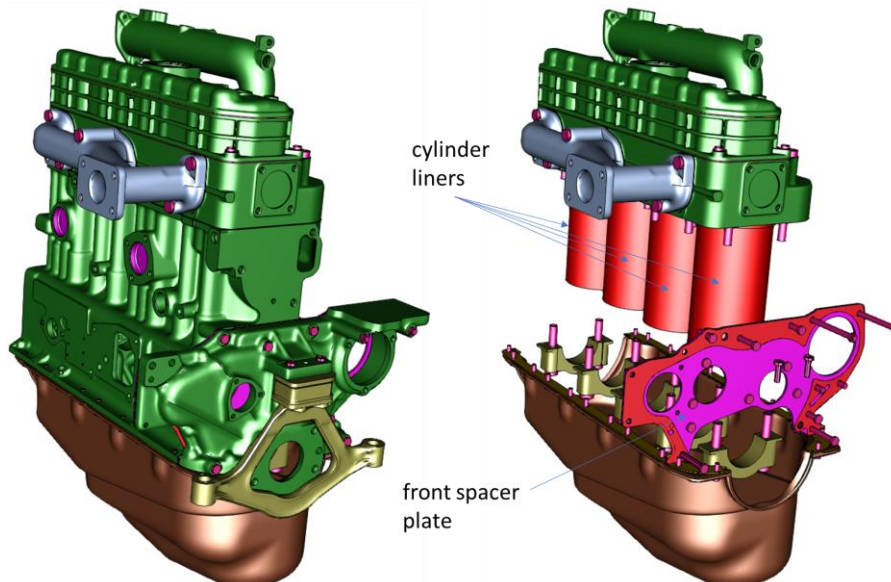


Fig.2: Exterior and interior (left image) of the FE-model. Solid element formulation -18 is used in the cylinder liners (four red parts) and front spacer plate (purple).

2.2 Material models

For modelling thermomechanical fatigue and cyclic plasticity, a non-linear mixed hardening material model due to Chaboche [12] is often applied in combustion engine analyses, see for example Ref.

[15]. This material model is available in LS-DYNA as ***MAT_DAMAGE_3**, which now has been augmented to allow temperature dependent material parameters. Typical responses under cyclic loading are illustrated in Fig.3:. In this demonstration, ***MAT_DAMAGE_3** with the newly developed temperature dependence is used in the engine block, cylinder head and exhaust manifold.

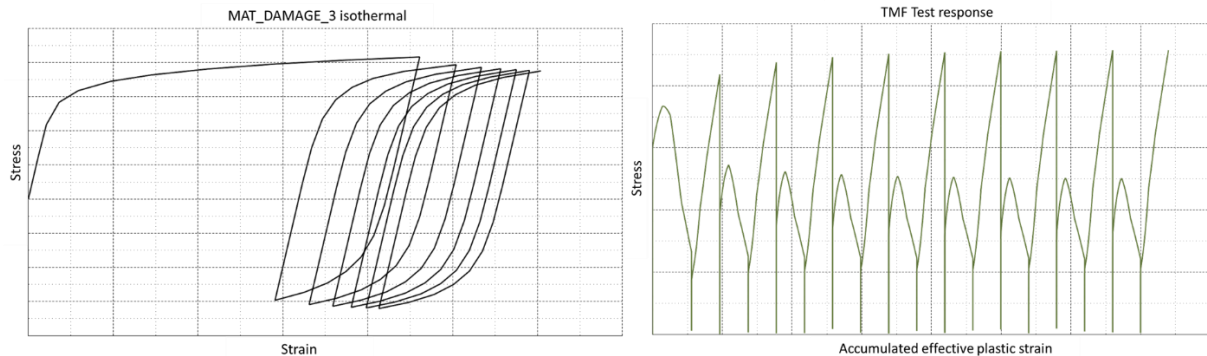


Fig.3: Typical behavior for the non-linear kinematic hardening model of ***MAT_DAMAGE_3**. The left image shows strain cycling at constant temperature. The right image shows the response under a TMF test, where both strain and prescribed temperature is varied simultaneously.

It was assumed that the engine block, cylinder head, intake manifold, front cover and valve covers (green in Fig.2:) are made from cast aluminum. The same material ID, with parameter values approximately corresponding to aluminum, was applied to these parts. Parameter values were estimated, inspired by for example Ref. [13] [14]. The temperature dependent hardening was estimated by simply scaling a master curve for temperatures from 25°C – 500°C, see the left image of Fig.4:. The yield stress drops after 150 °C and is significantly reduced above 260 °C.

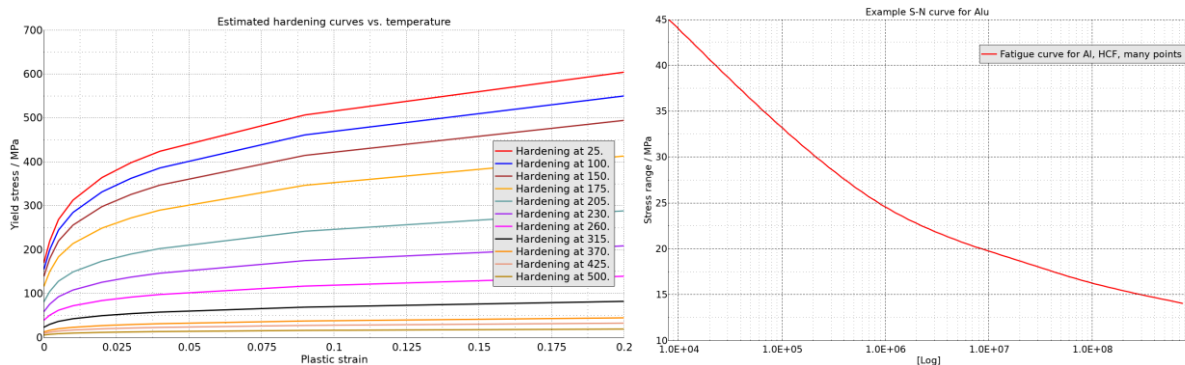


Fig.4: Left image: Estimated hardening curves vs. temperature, for the aluminum applied to the cylinder head and engine block. Right image: Example S-N curve for demonstrational purposes, from Ref. [18].

For a basic demonstration of the built-in fatigue analysis capabilities of LS-DYNA (see also for example Refs. [8][9]) a simple S-N curve for the aluminum was specified using the keyword ***MAT_ADD_FATIGUE**, see the right image of Fig.4:.

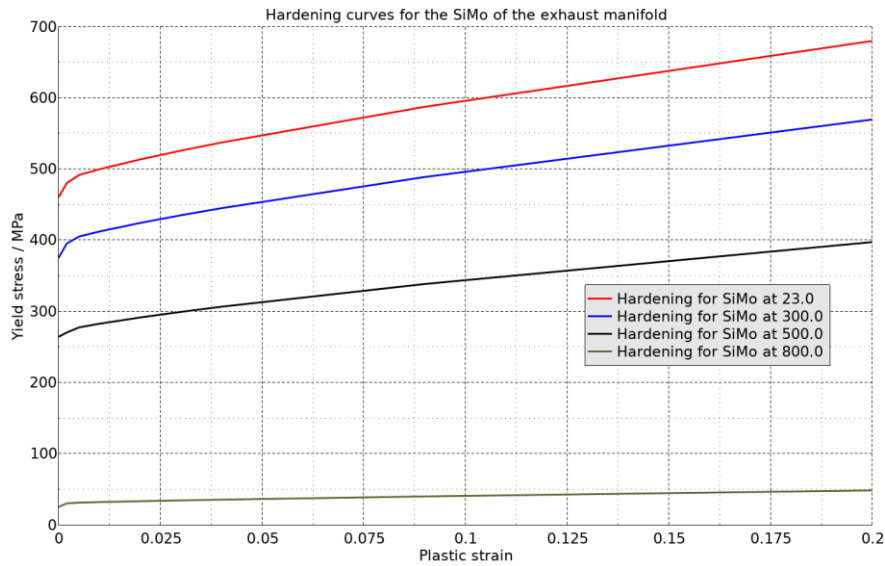


Fig.5: Estimated hardening curves vs. temperature, for the SiMo material applied to the exhaust manifold.

For the SiMo nodular cast iron in the exhaust manifold (gray in Fig.2:), temperature dependent parameters inspired by Ref. [16] were used for ***MAT_DAMAGE_3**. The hardening curves used for different temperatures are shown in Fig.5:. For this material, the yield strength drops noticeably between 500°C and 800°C.

The newly developed gasket material model, ***MAT_COHESIVE_GASKET**, was applied to the sump gasket, exhaust manifold gasket and cylinder head gasket. The gasket thickness is specified by the variable *gaskett* of ***SECTION_SOLID** when using solid cohesive element formulation 19. The ***MAT_COHESIVE_GASKET** allows for a meso-level description of gaskets and seals, where the gasket behavior is characterized by pressure vs. closure curves for loading and unloading, see Fig.6: for an example.

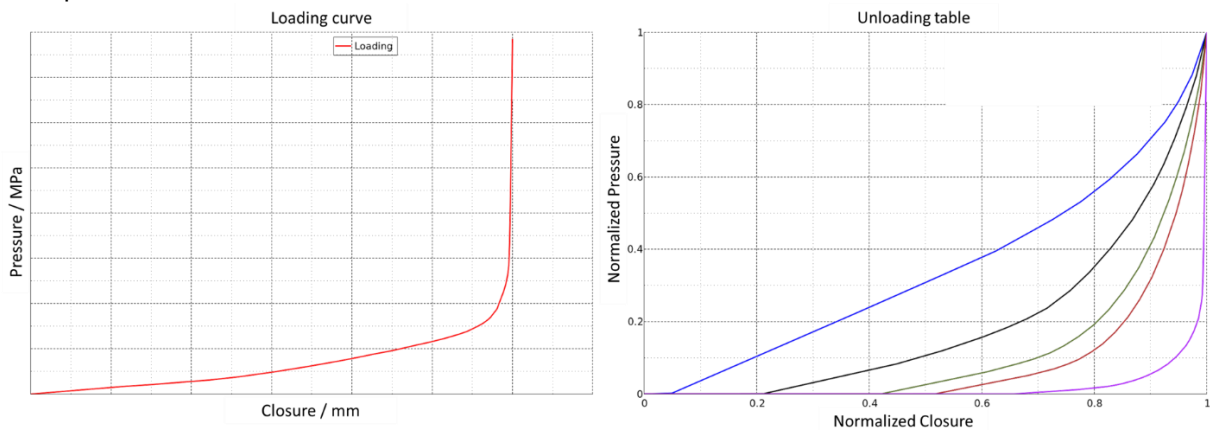


Fig.6: The pressure-closure relation for the gasket elements is defined by a loading curve (left image) and an unloading table (right image), using ***MAT_COHESIVE_GASKET**.

A new material model for polymer materials [17], including tension/compression asymmetry and a variable plastic Poisson's ratio (***MAT_SAMP_LIGHT**) is applied for modelling plastic parts of the oil pan (brown in Fig.2:). Temperature dependent material parameter remains to be implemented for this material model.

The remaining parts (bolts, cylinder liners, main bearing caps etc.) were assigned elastic material properties with temperature dependent Young's modulus. see Table 2: for an overview.

Table 2: Overview of material assignment

Mid	MAT_	Used in	Comment
65	187L	Oil sump	SAMP Light
88	1	Bolts	Elastic steel
112	106	Cylinder liners	Elastic (gray cast iron)
210	106	Spacer plates, washers, etc.	Generic steel (elastic)
500	153	Exhaust manifold	SiMo, Chaboche
727	4	Bottom bracket caps, front engine mount	Elastic, corresponding to Nodular Cast Iron
5200	153	Cylinder head, engine block, front cover	Aluminum, Chaboche
2002	326	Cylinder head gasket	

For the thermal load case, constant thermal conductivity, and specific heat with characteristic values for to each material, respectively, was assigned by use of `*MAT_THERMAL_ISOTROPIC`.

2.3 Contacts

Totally 17 contact definitions were used in the model, 3 sliding and 14 tied contacts. For the sliding contacts in the model, the Mortar formulations (`*CONTACT_AUTOMATIC..._MORTAR_ID`) were used. The gaskets were connected to the adjacent parts using tied contacts. Separate slave node sets and tied contact definitions for the gasket (cohesive) element top and bottom sides were used, to avoid the risk of “cross-constraining” and inverting these elements.

For the thermal analysis, the corresponding `_THERMAL` option on the contacts was activated.

3 Load case description

First a thermal-only load case was performed using estimated heat transfer coefficients to obtain a temperature distribution, see Section 3.1 for details, which then was used as a loading in the mechanical analysis (Section 3.2).

3.1 Thermal load case

The objective of the thermal load case was to obtain a reasonable temperature distribution, which could be used later on as a load in the mechanical analysis sequence. A steady state thermal analysis was performed using convection boundary conditions. Heat transfer coefficients (HTC:s) and ambient temperatures for the different surfaces were estimated and adjusted in order to obtain a desired temperature field, see Fig.7:.. In addition to the surfaces shown, convection boundary conditions were also applied to the outside of the engine, the inside of the valve cover, and the inside of the engine block. In a proper engine analysis, the HTC:s and corresponding temperatures would be obtained from an engine CFD analysis of the gas exchange cycle and coolant flow, something that would be possible using the CFD solvers of LS-DYNA. The nodal temperature results of the steady state analysis were extracted and applied in stages ii) and iv) – v) of the mechanical load case using `*LOAD_THERMAL_VARIABLE_NODE`, see further Section 3.2.

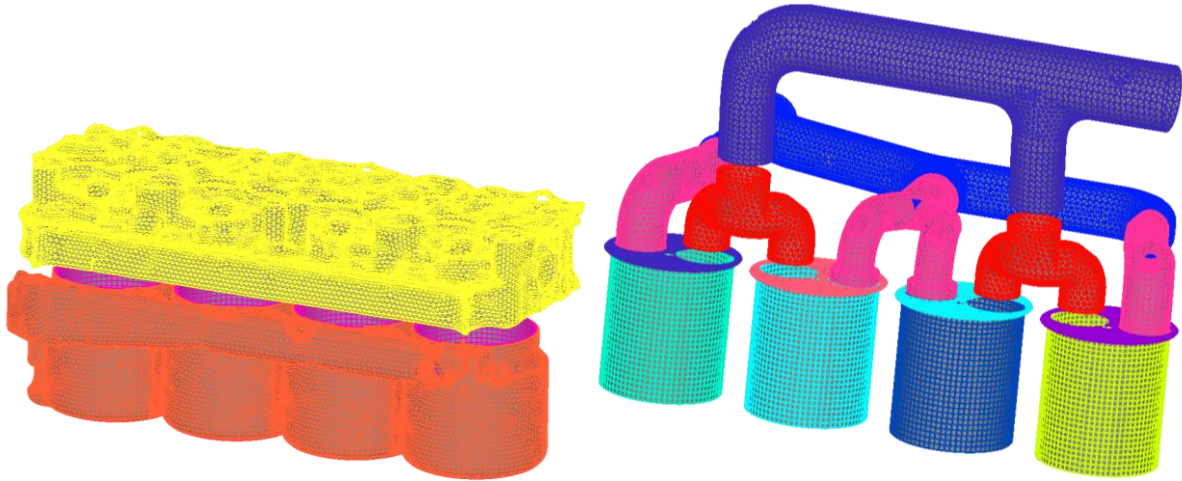


Fig.7: Segment sets for convection boundary conditions. The left image shows the coolant jacket of the cylinder head (yellow) and engine block (orange). The right image shows the surfaces facing the combustion gases (intake, cylinder liner, and exhaust).

3.2 Mechanical load case

The sequence of analyses for the mechanical load case consists of five stages:

- i) pre-tension of bolts,
- ii) one thermal load cycle (ramp up-down),
- iii) re-application of bolts pre-tension (see Table 3:),
- iv) ramp-up of thermal loading, and finally
- v) application of the cylinder pressure history.

The analysis sequence was set up as a series of separate analyses. The information was propagated through the analysis chain (see Fig.8:) using `dynain.1sda` – files, containing stresses, plastic strain and other history variables, but also contact state and other relevant information from the preceding stages, as described in Ref. [4]. The `dynain.1sda` – files contain the resulting configuration after each load stage, respectively, and can be re-used to create alternative load cases, for example if an alternative cylinder pressure is to be analyzed, only stage v) needs to be re-run.

Table 3: Bolt pre-tension forces

Bolt	Force / kN		Reduction
	Stage i)	Stage iii)	
Main bearing cap	87	70	-20 %
Oil pan	10	8	-20 %
Cylinder head	67	50	-25 %
Front cover	15	12	-20 %

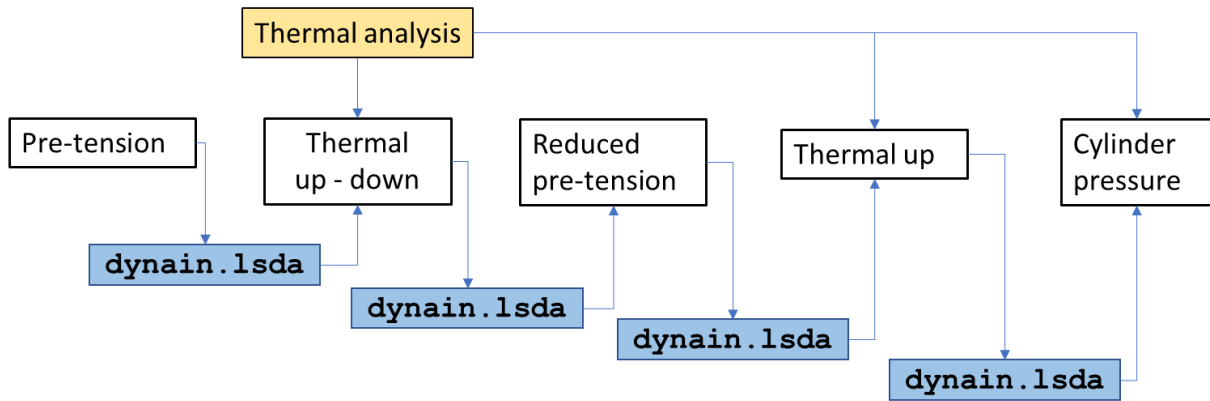


Fig.8: Analysis chain for the mechanical load case. The information is propagated using *dynain.lsd* – files. Temperature loading from the thermal analysis is applied to stage ii), iv) and v).

The analyses were set-up using the recommended settings of Ref. [6] without any specific modifications. Analyses ii) – v) were run as quasi-static, while i) starts out as dynamic to handle the initial rigid body modes of the assembly before the pre-tension is applied but ends as static. In all stages, constrained boundary conditions are applied to node sets at the front engine mount and two bolt holes at the back plate of the engine block.

The bolt pre-tensioning was applied using the keyword **INITIAL_STRESS_SECTION*, and the option *kbend = 2*, meaning that the bending stiffness of the bolts is accounted for. The re-application of bolt pre-tension to a reduced force, applied in stage iii), is another new feature for LS-DYNA: if there exists a prestress in the bolt, the stress is adjusted to meet the prescribed stress, even if it means reducing the stress. The load curve controlling the stress should start at the origin, just as for a normal pre-tensioning.

The stage v) of the mechanical loading consists of the cylinder pressure history, see Fig.9.:, for a complete firing cycle (assumed firing order cylinder 1-3-4-2), applied to the cylinder head and cylinder liner, with corresponding reaction loads being applied to the main bearing caps (also as distributed pressure). The full crankshaft dynamics was not considered for this load case.

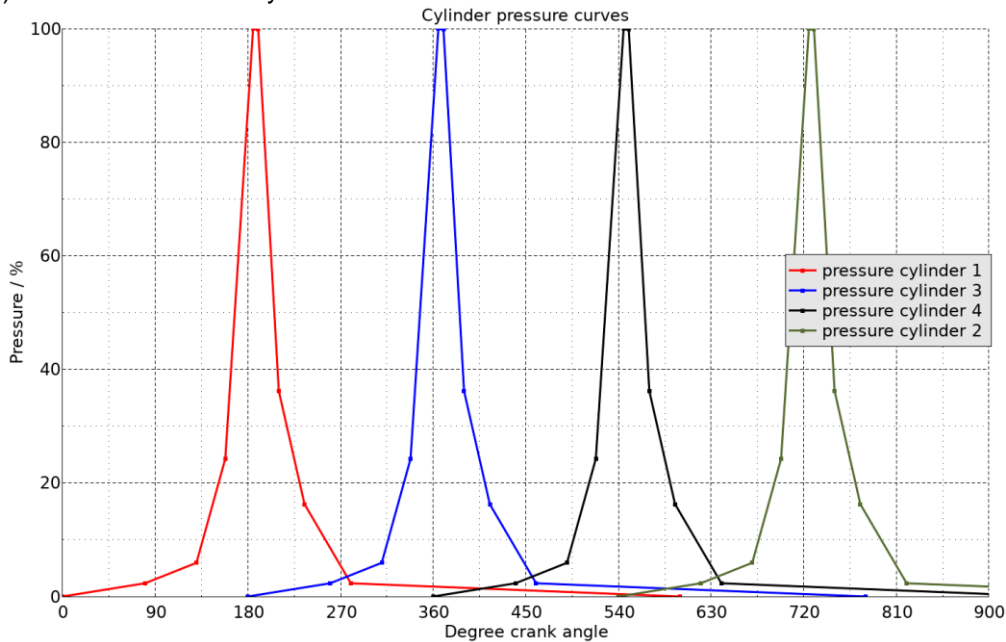


Fig.9: Assumed curves defining the (relative) cylinder pressure vs. crank angle history.

The cylinder pressure acting on the inside of the cylinder liner was applied using the keyword **LOAD_EXPANSION_PRESSURE*, by which the cylinder pressure can be applied to the part of the liner above the piston, see Fig.10:.. The peak cylinder pressure was estimated to be 18 MPa (180 bar) [19] .

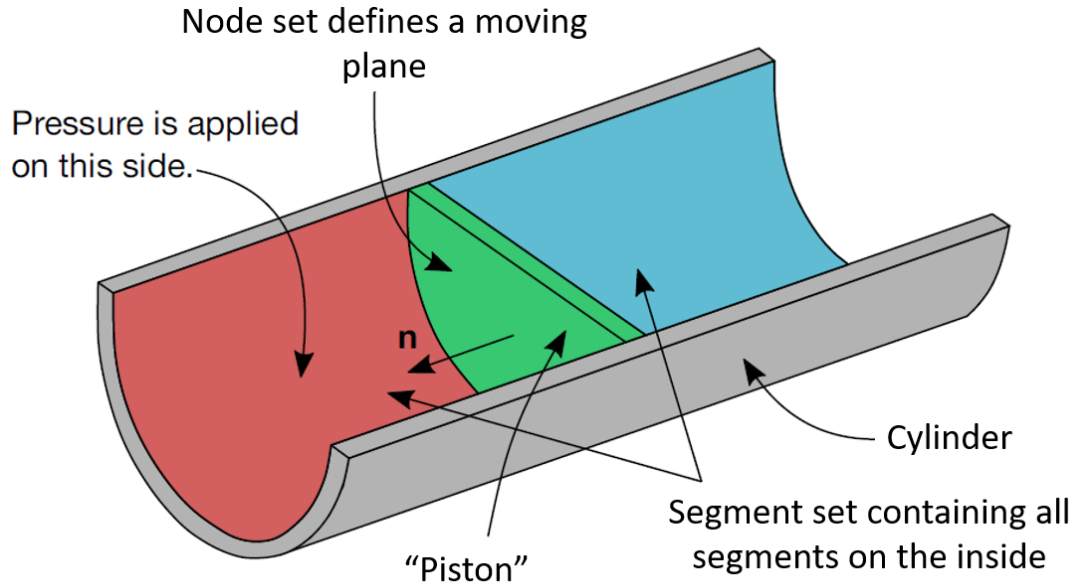


Fig.10: The keyword `*LOAD_EXPANSION_PRESSURE` is used for applying the cylinder pressure above the moving “piston” only. The moving plane (“piston”) is defined by a node set and a normal. Image from Ref. [5].

4 Results

In this section, some examples of analysis results are given. In Section 4.1, results of the steady state thermal analysis are shown. In Section 4.2, the results of the mechanical analysis are presented.

4.1 Thermal load case

The temperature distribution, in °C, is shown in Fig.12: for the complete assembly and in Fig.11: for the cylinder head.

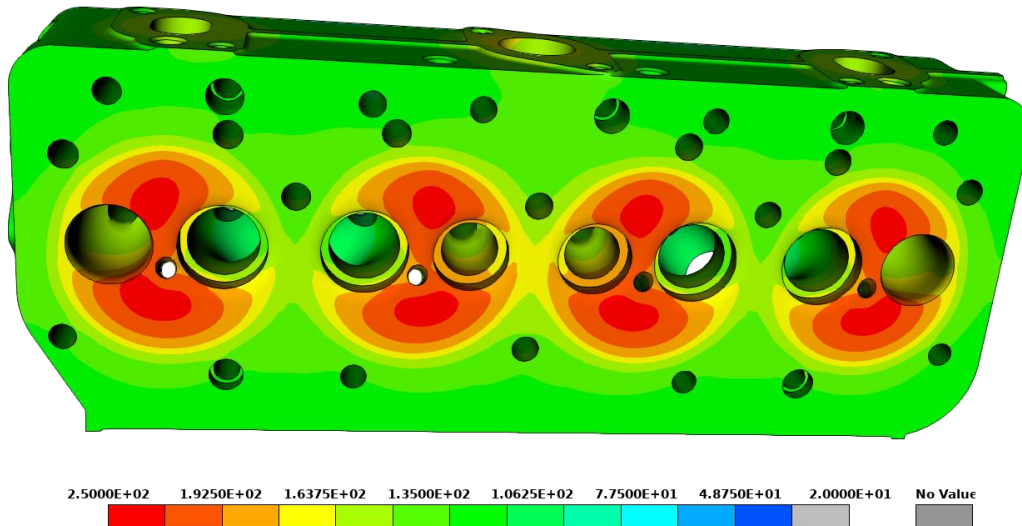


Fig.11: Temperature distribution in (in °C) the cylinder head. A peak temperature of about 260°C is reached.

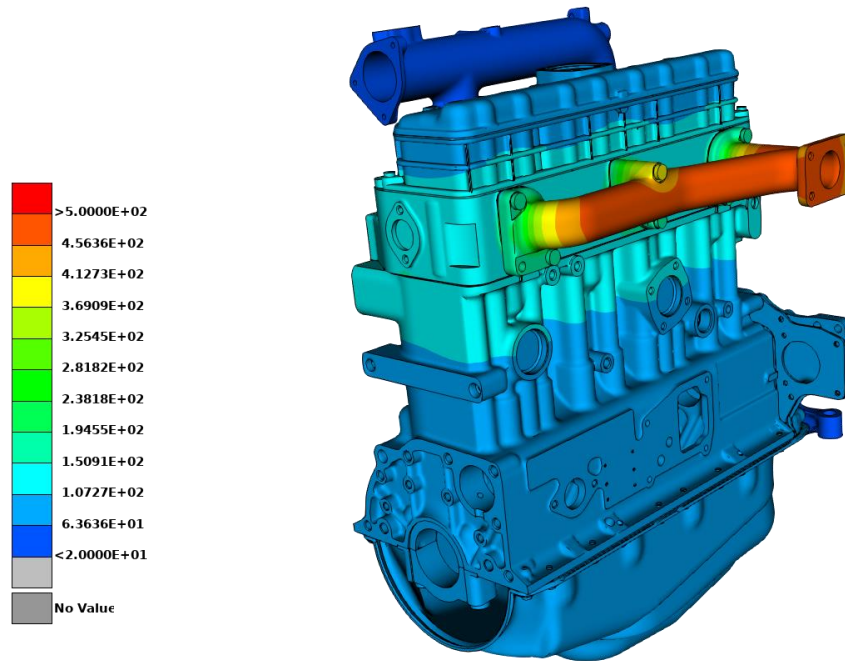


Fig.12: Temperature distribution (in °C) in the engine model. The exhaust manifold is the part with highest temperature (about 500°C).

4.2 Mechanical load case

A full-scale FE-analysis of a combustion engine gives results useful for many elements of engine design, for example:

- deformations, useful for evaluating bore distortion and valve alignment,
- stresses and strains in the different parts, useful for further fatigue analyses,
- forces in bolts, useful for fatigue evaluations,
- contact pressure and slip, useful for evaluation of risk for fretting, and
- gasket deformation and pressure, useful for evaluating the risk for leakage.

In this section, only a few examples are given of the possible results that could be extracted from the analysis. The peak effective stress (von Mises) during the cylinder pressure loading is shown in Fig.13:. The accumulated effective plastic strain in the cylinder head at the end of the analysis is shown in Fig.14:. The cylinder head gasket pressure is shown in Fig.15:, where the minimum values are noticeable low in the present simulation. This could indicate a risk for loss of sealing function. The variation in force in the bottom bracket bolts (dimension M16) is shown in Fig.16:. The mean force amplitude in the bolts is about 3.6 kN during the cylinder pressure loading, which would correspond to a stress amplitude of about 23 MPa.

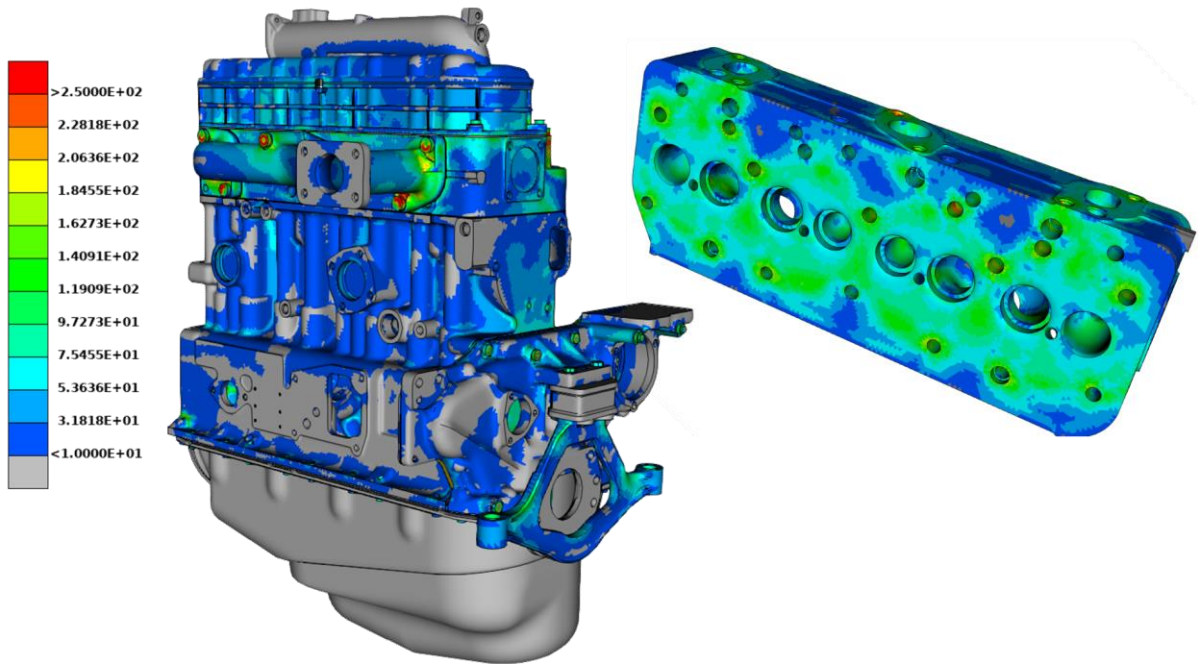


Fig.13: Peak von Mises stress during the cylinder pressure loading. The left image shows the complete assembly. The right image shows a detailed view of the cylinder head.

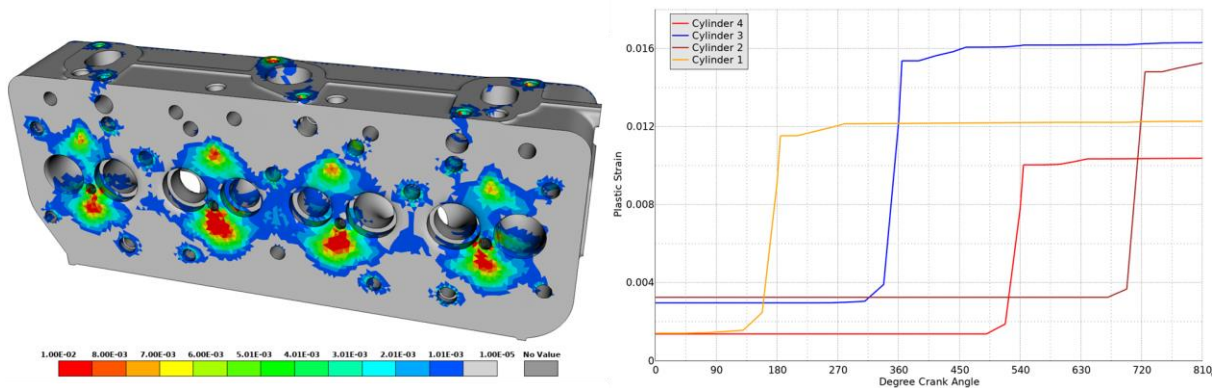


Fig.14: The left image shows the accumulated effective plastic strain at the end of the cylinder pressure loading. The right image shows the evolution of plastic strain at the combustion surfaces of cylinders 1 – 4.

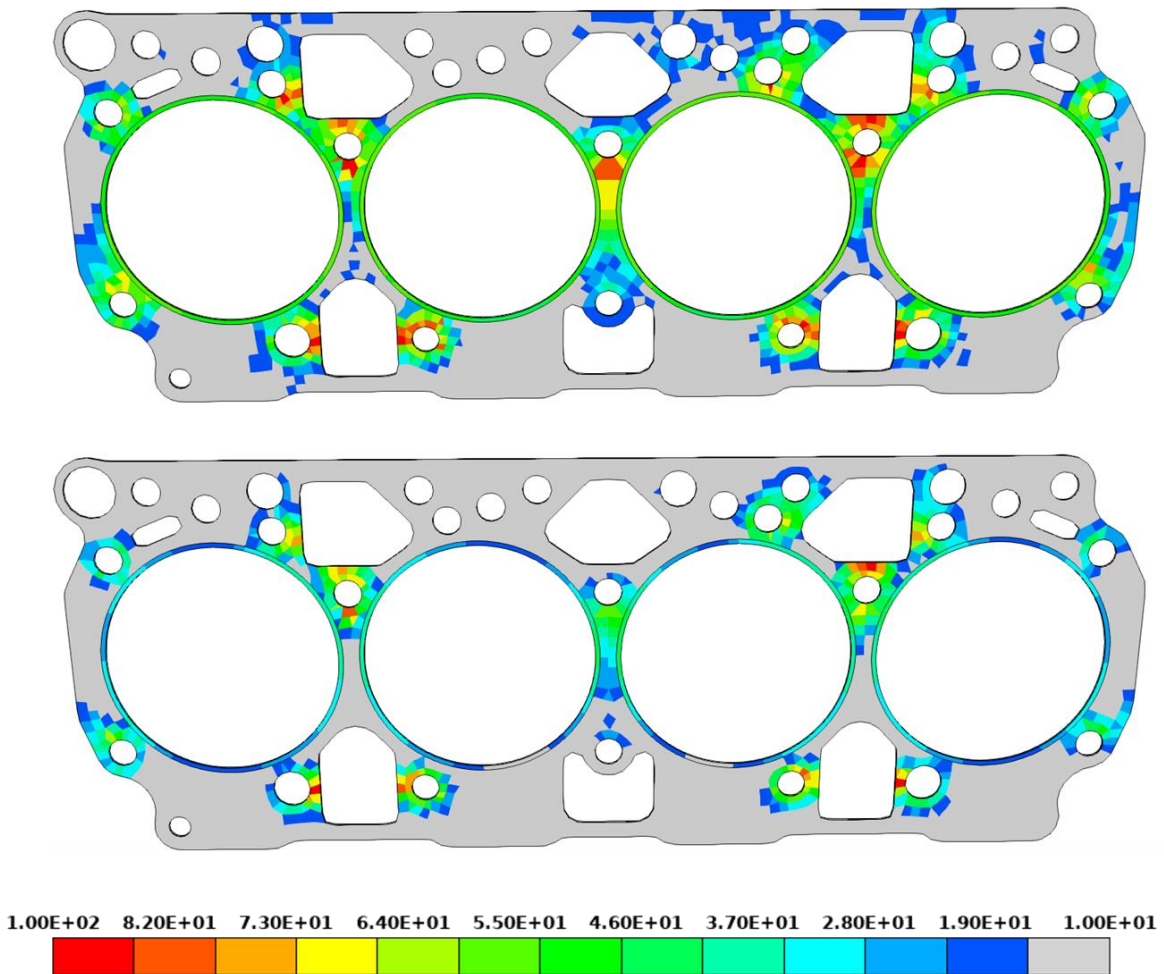


Fig.15: Gasket pressure. The top image shows the peak value during the cylinder pressure loading, and the bottom image shows the minimum value.

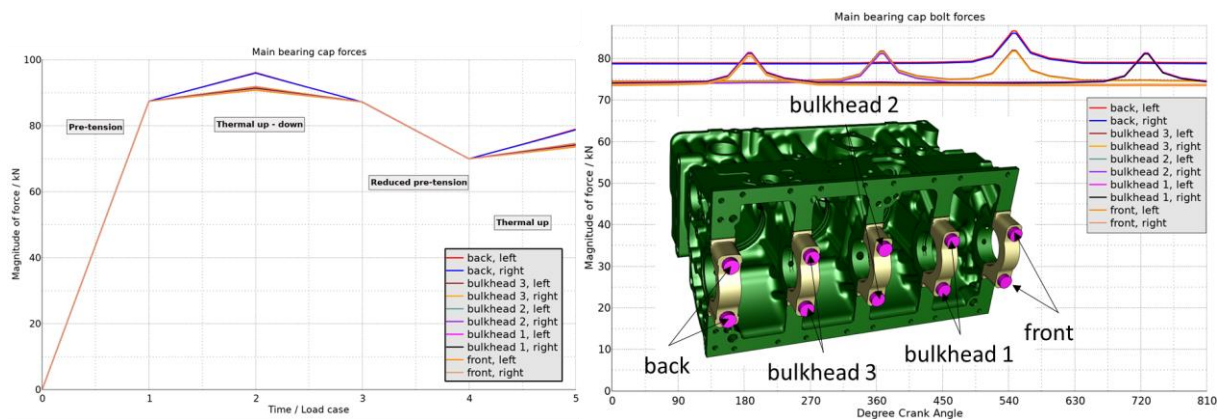


Fig.16: The left image shows the bolt force history during stages i) – iv). The right image shows the bolt force history during the cylinder pressure loading (stage v).

Finally, a basic High Cycle Fatigue analysis, based on the cylinder pressure history, was performed, using the *FATIGUE_ELOUT keyword. The fatigue damage is shown in Fig.17:.

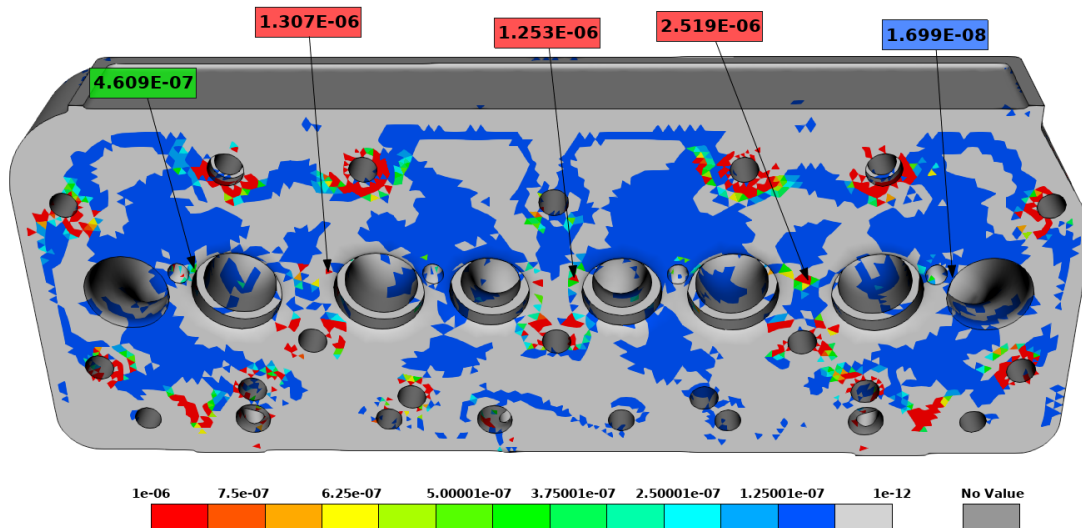


Fig.17: Fatigue damage due to the cylinder pressure history.

5 Summary

The development of the implicit solver of LS-DYNA is continuously progressing towards increased applicability. New material models and element types are added, and existing features are extended. In the presented case-study, a large-scale FE-analysis of a combustion engine was presented, as a demonstration of many recent enhancements:

- ***MAT_DAMAGE_3**, a Chaboche – type material model for cyclic plasticity with non-linear mixed hardening, now also with temperature dependent material parameters,
- New functionality for modelling gaskets, using cohesive elements and the new material model ***MAT_COHESIVE_GASKET**,
- New enhanced strain hexahedral element with incompatible modes (sold element formulation -18),
- ***MAT_SAMP_LIGHT**, the implicit implementation of a new material model for plastics,
- the ***CASE** and **dynain.lsda** – concept for multistage analyses,
- the added possibility of reducing bolt pre-tension by ***INITIAL_STRESS_SECTION**,
- and finally fatigue analysis by the keywords ***MAT_ADD_FATIGUE** and ***FATIGUE_ELOUT**.

The present demonstration shows that LS-DYNA implicit is well capable of solving difficult problems, involving large models, advanced material models and contacts. Hopefully the development will continue to make LS-DYNA implicit even more attractive in future versions.

6 Literature

- [1] Frondelius, T., Tienhaara, H., and Haataja, M.: “History of structural analysis & dynamics of Wärtsilä medium speed engines”, *Rakenteiden Mekaniikka (Journal of Structural Mechanics)* **51**:2, 2018, 1–31
- [2] Huang, Y., Kondapalli, P. S., and Jankowiak, T.: “Application of LS-DYNA to NVH solutions in the automotive industry”, 14th International LS-DYNA Conference, 2016
- [3] Ashcraft, C., et al.: “Increasing the scale of LS-DYNA implicit analysis”, 15th International LS-DYNA conference, 2018
- [4] Borrvall, T., et al.: “Solution Explorer in LS-PrePost – a GUI for non-linear implicit FE”, 12th European LS-DYNA Conference, 2019
- [5] Livermore Software Technology: “LS-DYNA keyword user’s manual Volume I”, Livermore 2021
- [6] Jonsson, A.: “Guideline for implicit analyses using LS-DYNA”, DYNAmore Nordic, 2021
- [7] Lilja, M., and Jonsson, A.: “Fatigue analysis based on complete machinery simulation – current and future features”, NAFEMS Nordic seminar, 2019
- [8] Lilja, M., “Time domain fatigue analysis in LS-DYNA R12”, DYNAmore Nordic, 2020

- [9] Huang, Y., Jonsson, A., and Lilja, M.: "Multiaxial fatigue analysis with LS-DYNA", 16th International LS-DYNA conference, 2020
- [10] Slyusarev, A., personal communication 2021-05-04
- [11] BETA CAE SA, ANSA Users Guide, Version 20.X, 2020
- [12] Lemaitre, J. and Chaboche, J.-L., "Mechanics of solids materials", Cambridge University Press, Cambridge 1990
- [13] Summers, T., et al., "Overview of aluminum alloy mechanical properties during and after fires", Fire Science Reviews 4, Article number 3(2015), internet source: <https://firesciencereviews.springeropen.com/articles/10.1186/s40038-015-0007-5>
- [14] Internet source: Engineering Toolbox, https://www.engineeringtoolbox.com/young-modulus-d_773.html
- [15] Szmytka, F., et al., "Some recent advances on thermal-mechanical fatigue design and upcoming challenges for the automotive industry", *Metals* **2019**, 9(7), 794, internet source: <https://www.mdpi.com/2075-4701/9/7/794/html>
- [16] Internet source: <http://www.iron-foundry.com/SiMo-Ductile-Iron-Chemical-Properties-Exhaust-Manifold.html>
- [17] Helbig, M., et al., "Characterization and material card generation for thermoplastics", 16th International LS-DYNA Conference, 2020
- [18] Dressel, A., English Wikipedia, CC BY-SA 3.0, internet source: <https://commons.wikimedia.org/w/index.php?curid=6319461>
- [19] Eilts, P., Stoeber-Schmidt, C., and Wolf, R., "Investigation of Extreme Mean Effective and Maximum Cylinder Pressures in a Passenger Car Diesel Engine," SAE Technical Paper 2013-01-1622, 2013, <https://doi.org/10.4271/2013-01-1622>